Development of Wall-Climbing Robot Using Vortex Suction Unit and Its Evaluation on Walls with Various Surface Conditions

Jianghong Zhao and Xin Li[(✉)]

State Key Lab of Fluid Power Transmission and Control, Zhejiang University,
38 Zheda-Road, Hangzhou 310027, Zhejiang, People's Republic of China
{zhaojianghong,vortexdoctor}@zju.edu.cn

Abstract. This paper presents a wall-climbing robot called Vortexbot, which has a suction unit that uses vortex flow to generate a suction force. Unlike the traditional unit based on contact-type adsorption, the suction unit does not touch the wall surface, which greatly reduces the frictional resistance between the robot and wall and improves the passing ability of the robot. It first introduces the principle of the vortex suction unit. Then, the authors design the mechanical structure of Vortexbot. Furthermore, they survey the suction properties of the suction unit on a smooth wall surface. In addition, they study the effect of the roughness and shape (a raised obstacle and groove) of the wall surface on the suction performance of the suction unit. Finally, they experimentally verify the climbing performance of Vortexbot on several kinds of walls with different surface conditions.

Keywords: Climbing robot · Vortex suction unit · Non-contact gripping · Rough surface · Raised obstacle · Groove

1 Introduction

Today, robots play a major role in boosting industrial production and improving the quality of human life. Robots can replace humans in carrying out many dangerous and difficult tasks. A kind of specialised robot, the wall-climbing robot, has been widely used. Zhang H. et al. developed a series of climbing robots called Sky Cleaner I, II, III, and IV, which can clean the glass walls of high-rise buildings [1, 2]. NINJA I and II and ROMA I and II can carry out facade inspection and maintenance of high-rise buildings and bridges [3–6]. Roboclimber, a 3-ton spider robot, can autonomously execute slope consolidation tasks [7]. Alicia 1 and 2 can inspect equipment in petro-chemical plants [8]. ROBICEN III and Robug II can carry out facade inspection and maintenance in nuclear plants [9, 10]. REST can carry out inspection, cleaning, and welding tasks in a ship hull [11]. Undoubtedly, with the development of technology, climbing robots will be able to accomplish more tasks for human beings.

During the research and design of climbing robots, one of the issues that researchers mainly consider is the type of suction method to be used [12, 13]. Vacuum adsorption is the most commonly used method [1, 2, 14–16]. It mainly generates negative pressure in the suction cup to provide suction force for climbing robots. This method has the

following advantages. It can be used on walls of different materials. Its structure is relatively simple and can be manufactured easily at low cost. Existing vacuum technology can produce negative pressure close to full vacuum (i.e. 0 kPa (abs)); hence, theoretically, the suction cup can provide a large suction force, which can enable the robot to have a very strong load capacity. However, it is necessary to ensure very good sealing between the suction cup and wall surface to maintain the suction force. Otherwise, leakage might occur, which might lead to the failure of adsorption and might cause the robot to drop off the wall. This limitation restricts the use of the robot to walls with smooth and flat surfaces. Many researchers have adopted different approaches to overcome this problem (Fig. 1). Yanzheng Zhao et al. developed a wall-climbing robot with a single suction cup and adopted an air spring–regulating spring combination as the sealing mechanism (Fig. 1a) [17]. This mechanism enables the robot to work well on both glass and ceramic-tile surfaces. Longo D. et al. developed the second generation of the robot Alicia (Alicia 2) by using a larger cup, a much more powerful aspirator, and a sealing structure made by sandwiching Teflon and bristles (Fig. 1b) [8]. Therefore, Alicia 2 can work in much harsher environments such as a rough metal surface or concrete wall. Cromsci, developed by Schmidt D. et al., has a seven-chamber adhesion system and an adaptable inflatable rubber sealing (Fig. 1c); its surface is made of synthetic fibres, which make it suitable for large vertical concrete buildings [18]. Mo Koo et al. proposed a wall-climbing robot called LARVA, which contains an impeller-type adhesion mechanism [19]. To maintain the suction force, the robot uses a double-layered sealing mechanism consisting of a flexible bending layer and single straight layer (Fig. 1d). This mechanism allows it to climb rough concrete walls.
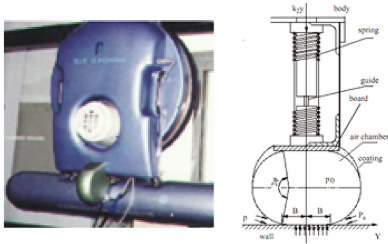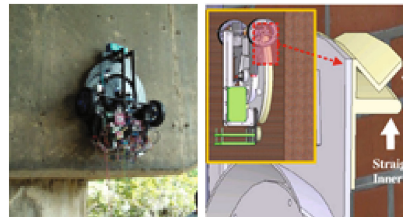

(a) Robot (left) and its sealing mechanism (right), developed by Zhao et al. [17]
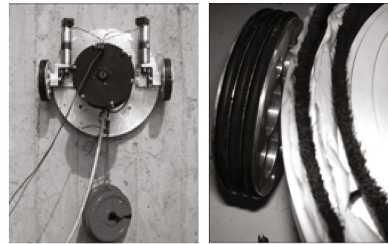
(b) Alicia 2 And its sealing mechanism [8]
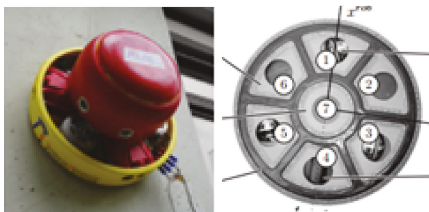
(c) Cromsci and its seven-chamber adhesion system and an adaptable inflatable rubber sealing[18]

(d) LARVA and its double-layered sealing mechanism [19]

Fig. 1. Wall-climbing robots with sealing mechanisms, which enable robots to climb walls with relatively rough surfaces

The abovementioned studies based on existing technology indicate that the most widely used method used for suppressing the leak between the suction cup and wall surface is to design and strengthen the sealing mechanism. However, while climbing a wall, the robot is influenced by the frictional resistance between the wall surface and the various kinds of complex sealing mechanisms. To ensure good sealing, the robot has to withstand a large frictional resistance because the frictional resistance is always in conflict with the sealing effect [20, 21]. In addition, the frictional resistance can cause the abrasion of the sealing material and simultaneously limit the walking speed of the robot because of the deformation of the sealing parts. Furthermore, because the actual nature of a wall surface can be very complex, the sealing mechanism cannot always ensure that it is close to the wall surface, which can lead to fluctuations in the suction force and hence hamper the smooth running of the robot [19]. We believe that it is very necessary and important to devise a new adsorption method that can avoid the series of problems encountered by vacuum suction methods.

2   The Suction Unit Based on Vortex Flow

Vortex levitation was proposed and studied by Li et al. in 2008 [22], and it has been used to develop a new kind of non-contact gripping mechanism [22–24]. The vortex gripper (Fig. 2) is mainly composed of a cylindrical vortex chamber and two tangential nozzles, which are created on the circular wall of the chamber. The compressed air blows into the vortex chamber through the tangential nozzles and forms a high-speed vortex flow along the internal face of the chamber. As in the case of a tornado, the centrifugal force produced by the vortex flow pushes the air in the center towards the peripheral region of the chamber, and thus, a negative pressure zone with rarefied air is created at the center. As a result, a considerable pressure difference is created between the top and bottom surfaces of the workpiece, which is placed under the vortex gripper. That is, the workpiece experiences an upward suction force. When the negative pressure is sufficiently large, the suction force becomes larger than the gravity of the workpiece. At this point, the workpiece is lifted up. In addition, because compressed air is constantly supplied through the nozzles into the vortex chamber (blue arrows in Fig. 2), air is continuously vented through the gap between the gripper and workpiece. This exhaust flow ensures that the gripper and workpiece do not contact each other.
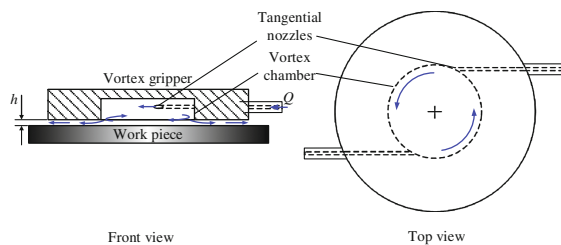

Fig. 2. Schematic of vortex gripper

3   The Proposed Wall-Climbing Robot, Vortexbot

We designed and manufactured a wall-climbing robot called Vortexbot (Fig. 3). It mainly consists of a car body and suction mechanism. It adopts the all-wheel-drive mode as the driving mode, which enables the robot to take full advantage of the suction force provided by the suction unit while climbing a vertical wall. Three wheels are installed on the based board of the car body and are driven by three geared DC motors. The suction unit is installed under the based board by screw connections. In addition, we ensure that the screw connections are located as close to the three wheels as possible. This design reduces the effect of force couples on the based board (i.e. the force couples formed by the counter force provided by the wall surface to each wheel and the suction force provided by the suction unit that spreads on each screw connection). Consequently, the design also reduces the strength requirement for the based board. Therefore, the based board is designed to be hollow in many sections, which makes the robot lightweight. A servomotor is used to change the direction of the front wheel and hence realise the steering motion of the robot. The drive circuit is installed on the based board and is used to control the movement of the robot. The robot is manufactured mainly using carbon fibre plate because it has both high strength and light weight.
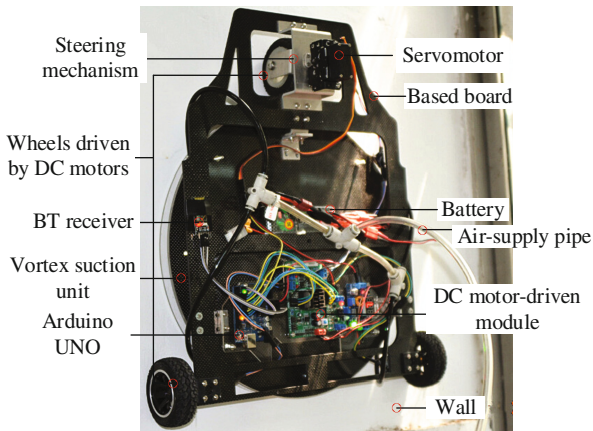
Fig. 3. Photograph of Vortexbot

According to the principle described in Sect. 2, we designed and manufactured the vortex suction unit (Fig. 4). Its specific dimensions (unit: mm) are indicated in the figure. The suction unit consists of a vortex ring (internal radius: 150 mm, height: 18 mm), an annular skirt (radius: 180 mm, height: 3 mm), an upper cover (radius: 160 mm, height: 2 mm), and four nozzles (diameter: 2 mm), which are tangentially and symmetrically distributed inside the chamber. Because the upper cover needs to bear the suction force, we used a high-strength carbon fibre plate. We used acrylic plates, which are lighter, to manufacture the vortex ring and annular skirt because these parts do not need to have high strength.
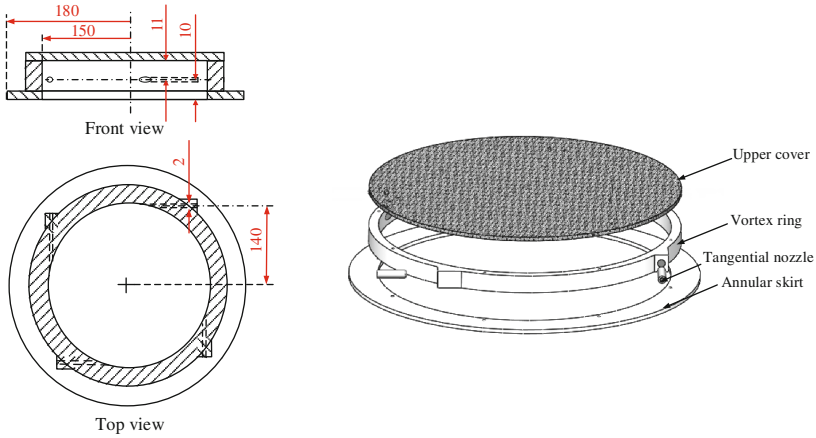
Fig. 4. Schematic structure and explosive view of vortex suction unit used in this study

4 Experimental Methods

4.1 Experimental Setup for Suction Force Measurement

We set up a measuring apparatus (Fig. 5) to study the change in the suction performance of the suction unit when the surface condition of the wall varies. The apparatus mainly consisted of two parts: a fixed trestle and a vertical mobile platform. The fixed trestle was used to fix the suction unit and force sensor, which was used to measure the suction force. The vertical mobile platform was set below the suction unit. We can install different simulated walls on the platform and change them. We can also adjust the distance between the platform and the suction unit by adjusting the feeding bolt. The following steps were performed during the experiment: (1) the vortex suction unit was fixed on the fixed trestle, and the simulated wall was installed on the vertical mobile platform; (2) the six leveling bolts were adjusted to ensure that the upper surface of the simulated wall just horizontally touched the lower surface of the suction unit; (3) the feeding bolt was adjusted to vertically lower the simulated wall and the distance between the simulated wall and the suction unit; (4) the gas switch was opened to provide compressed air at a certain flow rate to the suction unit; (5) a data acquisition card was used to record the change in the reading of the force sensor equal to the suction force and simultaneously obtain the distance value (i.e., h) from the screw micrometer on the lifting platform; and (6) steps 3–5 were repeated by adjusting h. We can obtain the $F–h$ curve (i.e., the curve of the suction force against the distance) for the suction unit on the simulated wall with a given surface condition using the above steps.

4.2 Experimental Setup for Pressure Distribution Measurement

The air movement in the vortex suction unit controls the pressure distribution. In other words, the pressure distribution reflects the flow state. Therefore, we studied the flow

state inside the vortex suction unit by measuring the pressure distribution. Figure 6 shows the pressure distribution measurement apparatus that we designed. We machined 37 pressure measuring taps on the upper cover of the suction unit. The front end of each tap had a diameter of 1 mm. The back end was connected to the pressure sensor using a tube with a diameter of 1.5 mm. Each tube as equipped with a switching valve. First, we closed all the valves to cut off the connection between the taps and the pressure sensor. We then installed the vortex suction unit on the apparatus shown in Fig. 5 in accordance with the steps listed in Section B. After which, we set the required experimental conditions. We opened one of the valves, connected the measuring tap to the pressure sensor, and recorded the sensor reading and the measuring tap location during the pressure distribution measurement process. We then closed the opened valve. We repeated the abovementioned steps to obtain the data corresponding to all the 37 measuring taps. We can finally determine the pressure distribution inside the vortex chamber (i.e., P–r curve) using this process.
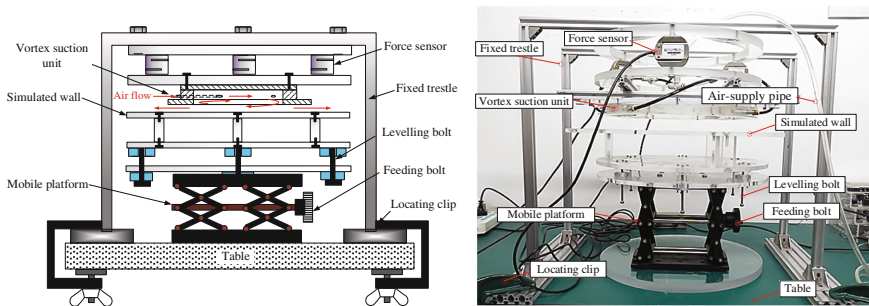

Fig. 5. Schematic and photograph of experimental setup used for measuring suction force
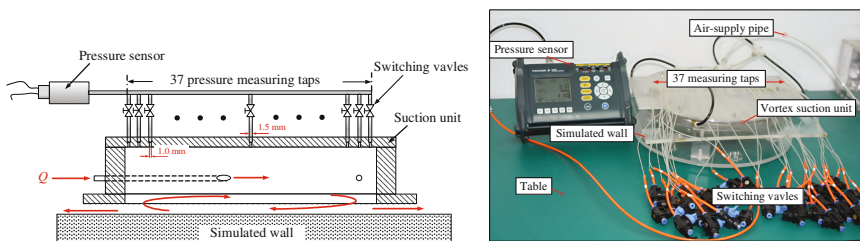

Fig. 6. Schematic and photograph of experimental setup used for measuring pressure distribution

5   Results and Discussion

5.1   Suction Performance of the Suction Unit on the Smooth Surface

We first obtained the F–h curve for the suction unit on a smooth surface. We obtained the F–h curves at different supply flow rates (Q = 200, 250, 300, 350, 400 L/min (ANR)) (Fig. 7). The suction force continuously increased as the flow rate increased. In addition, the changing trend of the F–h curves at different flow rates was almost the same. We rearranged the data in Fig. 7, as shown in Fig. 8, to more clearly express the tendency of change in the suction force when Q varies (i.e., F–Q curves). The variation tendency of the F–Q curves was almost the same when h changes. In addition, the F–Q curves can be well fitted by some quadratic curves. The correlation coefficient of each fitting curve was larger than 0.9953.
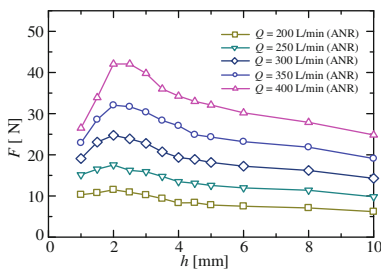

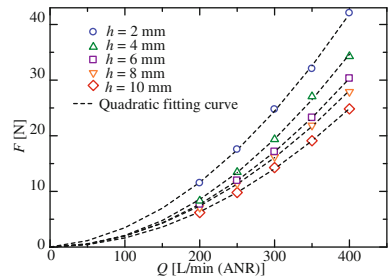**Fig. 7.** F–h curves for vortex suction unit at different supply flow rates

Fig. 8. F–Q curves for vortex suction unit at different distances

This relationship is strong evidence for the adjustment of the suction force by changing the supply flow rate. For example, consider a case, where the suction unit is fixed to the robot, such that the distance between the wall and the suction unit is constant. Suppose that the original supply flow rate is Q_0. The suction force F 0 is kQ_0^2, where k is the proportional coefficient. The percentage change in the suction force can be expressed as follows if we change the flow rate to Q_1, then the percentage change in the suction force can be expressed as

$$\frac{\Delta F}{F_0} = \frac{kQ_1^2 - kQ_0^2}{kQ_0^2} \times 100\% = \left[\left(\frac{Q_1}{Q_0} \right)^2 - 1 \right] \times 100\% \tag{1}$$

A simple functional relationship exists between the percentage change in the suction force and the supply flow rate. That is, if we want to increase/decrease the suction force to a certain percentage ($a\%$), we can use this relationship to obtain the value of the required flow rate (i.e. $Q_1(= Q_0\sqrt{(1 \pm a\%)})$). This relationship is very important for adjusting and controlling the suction force of the climbing robot.

5.2   Suction Performance of the Suction Unit on the Rough Surfaces

Vortexbot will encounter wall surfaces with different roughness during real climbing. We used several pieces of sandpaper to study the effect of different surface roughness on the suction force of the vortex suction unit and simulate wall surfaces with different roughness. Figure 9 shows a smooth surface (i.e., acrylic plate) and three kinds of rough surfaces (i.e., sandpaper with mesh numbers of 400, 120, and 60). The wall surface becomes rougher as the mesh number decreases. Figure 10 shows the suction force variation on wall surfaces with different roughness for a supply flow rate of 350 L/min (ANR) and h of 4 mm. The suction force became smaller as the surface became rougher. The amplitude of the suction force decreased by 28.2% compared to that for the smooth surface when the roughness was P 60. It shows that the rotation flow inside the vortex chamber was weakened by the rough surface because the rough surface produces a resistance to the rotation flow. Moreover, the rougher the surface, the larger the resistance, which leads to a decrease in the rotating speed of air and the suction force.
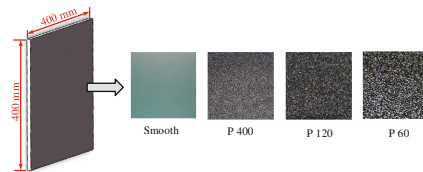

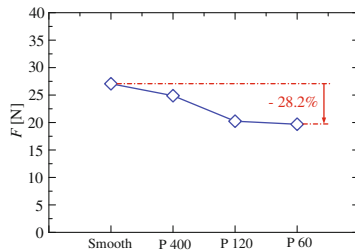
Fig. 9. Wall surfaces with different roughnesses

Fig. 10. Suction forces on wall surfaces with different roughnesses

5.3   Stepping Over Raised Obstacles

The process of the suction unit passing over a raised obstacle when Vortexbot walks on a wall surface with raised obstacles was a dynamic process. The climbing speed of the robot was almost negligible compared to the flow velocity of the rotating flow inside the vortex chamber. Hence, we can study such a dynamic process by studying the static pressure distributions and the suction forces when the raised obstacle was at different positions under the suction unit. Figure 11 shows the seven steps when the suction unit passes over a raised obstacle. Steps 1 and 7 represent the situations before and after the suction unit passes over the obstacle, respectively. Therefore, the wall surface under the
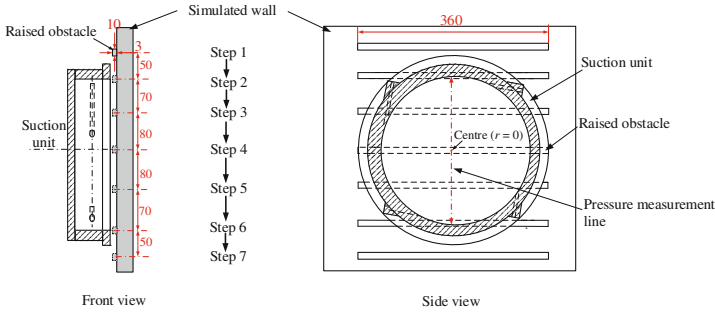
Fig. 11. Relative positions of obstacle and suction unit in different steps

suction unit at these two moments was smooth. Steps 2–6 represent different positions when the suction unit passes over the obstacle. The raised obstacle was 3 mm in height, 10 mm in width, and 360 mm in length.

Figures 12 and 13 show the variation in the suction force and pressure distribution, respectively, for every step. The suction performance of the suction unit was obviously affected when the suction unit passed over the obstacle. In step 1, the obstacle was outside the suction unit. At this moment, the suction force and the pressure distribution were the same as those on a smooth wall surface. In step 2, the obstacle was at the edge of the vortex chamber. Contrary to expectations, the suction force increased by 16%. The pressure distribution in step 2 indicated that the obstacle caused the negative pressure in the center of the vortex chamber to become lower than that in step 1. That means, the air rotation inside the suction unit became more severe at this moment, which might be because the obstacle can protect the rotation flow inside the vortex chamber when it was at the edge of the chamber.

Li indicated that air can easily discharge from the vortex chamber when the distance is large, which makes the air rotation inadequate and weakens the negative pressure distribution. We consider that the obstacle can prevent the air from being discharged from the chamber and can force the air to rotate in the chamber more adequately, which helps in the formation of a lower negative pressure distribution. The suction force considerably declines by 23% compared to the suction force in step 1
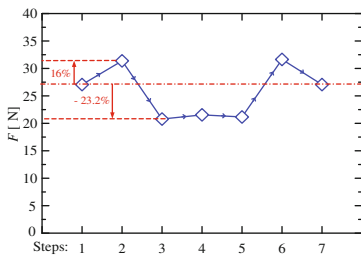

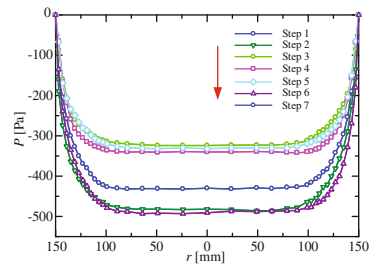**Fig. 12.** Fluctuation in suction forces in different steps

Fig. 13. P–r curves for different steps

when the obstacle reaches the position in step 3. Correspondingly, the negative pressure at the center of the chamber clearly increases. The obstacle hinders air rotation, which weakens the centrifugal effect of the rotation flow. The experimental data indicated that compared to step 3, the suction force and the pressure distribution were not affected by the movement of the obstacle when the obstacle as at the position in step 4. Accordingly, we observed nearly the same variation when the obstacle shifted out of the vortex chamber (steps 5, 6, and 7). In other words, the processes involved in the obstacle moving into and shifting out of the vortex chamber were symmetric.

The abovementioned analysis indicated that the relative positions of the obstacle and the suction unit can cause the suction force to fluctuate when Vortexbot steps over a raised obstacle on a wall surface. For the suction force to substantially decrease when the obstacle is inside the vortex chamber is dangerous. We should take some steps to counter such a situation (e.g., increase the supply flow rate to compensate for the decrease in the suction force or prevent the obstacle from entering the vortex chamber).

5.4   Stepping Over Grooves

As in the case of Fig. 11, we only replaced the obstacle by a groove. The groove was 3 mm in depth, 10 mm in width, and 360 mm in length. Figures 14 and 15 show the variation in the suction force and pressure distribution, respectively, in different steps. Compared to the raised obstacle (previous subsection), the groove had a much milder effect on the suction force and pressure distribution. The experimental results showed that the suction force slightly decreased when the groove entered the suction unit. The decrease in the suction force amplitude was within 10% compared to the suction force in step 1. In addition, the suction force almost remained constant when the suction unit passed over the groove, despite the change in the relative positions of the suction unit and the groove. We considered that this finding was obtained because the groove cannot hinder the rotation flow like the raised obstacle. Therefore, we only needed to slightly increase the supply flow rate when the robot steps a groove to ensure that the robot steadily passes over the groove.
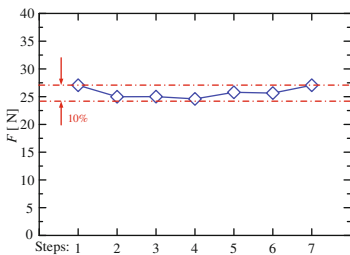

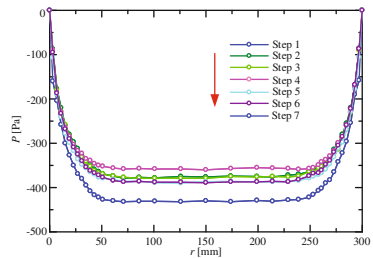**Fig. 14.** Fluctuation in suction forces in different steps

Fig. 15. *P–r* curves for different steps

6 Practical Climbing Experiments

6.1 Climbing on Walls with Different Obstacles

Figure 16 shows the scene, where Vortexbot stepped over some raised obstacles and the specific dimensions (unit: mm). The results confirmed the major contribution of the new suction unit in improving the ability of the climbing robot to pass over obstacles. We can find that Vortexbot can pass over obstacles with heights ranging from 5 mm to 15 mm, which shows the powerful passing ability of Vortexbot.

Fig. 16. Experiment on a smooth wall with raised obstacles

6.2 Payload Testing Experiment

We used dumbbells as the load to test the load capacity of Vortexbot (Fig. 17). The mass of Vortexbot itself (i.e., G_0) was 2388 g. The distance between the vortex suction unit and the wall surface was set as 2 mm. The suction unit only needed a supply flow rate (i.e., Q_0) of 330 L/min to make Vortexbot stably climb on the wall surface when the robot did not carry any payloads. We then gradually increased the payload (i.e., $G_t - G_0$) and the supply flow rate (i.e., Q). We obtained the $G_t - Q$ curve (Fig. 17(b)). We can see from the figure that: (1) Vortexbot can carry a payload with a mass of 2.5 kg when the supply flow rate was up to 484 L/min (the total mass of the robot at the moment was 4.888 kg ($G_t = 2.05\ G_0$)); and (2) the load capacity was in direct proportion to the square of the supply flow rate, which was consistent with the quadratic
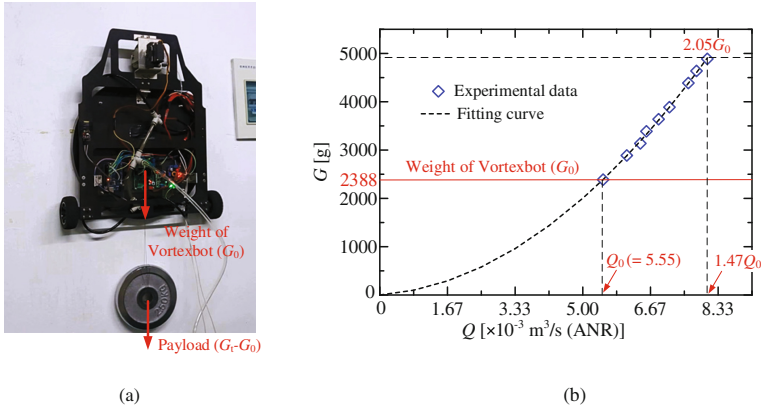
(a)   (b)

Fig. 17. Photograph and data of the payload experiment

curve of the suction force and the supply flow rate (Fig. 8), suppose the friction coefficient was unvarying. The result implied that the robot can have a larger load capacity by increasing the supply flow rate.

7   Conclusion

This study presents a climbing robot, called Vortexbot, which uses a vortex suction unit. This unit uses vortex flow to generate a negative pressure and provide a sufficient stable suction force. Unlike the traditional unit based on contact-type adsorption (vacuum suction), the vortex suction unit can maintain a certain distance between itself and the wall surface because of the existence of a gap for air discharging. Hence, this unit can realize a non-contact suction. Consequently, Vortexbot can adopt a wheel-driven locomotion to realize an efficient movement. Such a kind of suction mechanism needs no sealing mechanism to prevent vacuum leakage, which greatly reduces the frictional resistance between the robot and the wall. The compressed air vents from the gap between the suction unit and the wall surface after rotating in the vortex chamber. Hence, such kind of flow direction can avoid the effect of the dust and dropped items on the wall surface. As a result, Vortexbot can easily climb walls with various surface conditions, including surfaces that are rough, with raised obstacles, and with grooves. In this study, we obtained the effect of the supply flow rate, surface roughness, inclined condition, obstacles, and grooves on the suction unit performance based on the experimental results. We also tested Vortexbot on real wall surfaces. Moreover, we tested the payload capacity of Vortex.

The abovementioned results provide substantial evidence to justify a further study of the climbing robot. In the future, we intend to study the flow phenomenon inside the vortex suction unit by means of a flow field visualization and a numerical simulation. We hope to explain the reasons for the effect of the surface condition of the wall on the suction force from the viewpoint of hydromechanics. Moreover, we intend to continue

optimizing the suction mechanism design and improve the obstacle-crossing ability and stability of the robot.

References

1. Zhang, H., Zhang, J., Wang, W., Liu, R., Zong, G.: A series of pneumatic glass-wall cleaning robots for high-rise buildings. Ind. Rob. Int. J. **34**, 150–160 (2007)
2. Zhang, H., Wang, W., Zhang, J.W.: High stiffness pneumatic actuating scheme and improved position control strategy realization of a pneumatic climbing robot. In: IEEE International Conference on Robotics and Biomimetics, pp. 1806–1811. IEEE Computer Society (2009)
3. Hirose, S., Arikawa, K.: Coupled and decoupled actuation of robotic mechanisms. In: IEEE International Conference on Robotics & Automation, vol. 1, pp. 33–39. IEEE (2001)
4. Hirose, S., Nagakubo, A., Toyama, R.: Machine that can walk and climb on floors, walls and ceilings. In: Proceedings of the International Conference on Advances in Robotics, pp. 753–758 (1991)
5. Balaguer, C., Gimenez, A., Abderrahim, M.: ROMA robots for inspection of steel based infrastructures. Ind. Rob. Int. J. **29**(3), 246–251 (2002)
6. Resino, J.C., Jardon, A., Gimenez, A., Balaguer, C.: Analysis of the direct and inverse kinematics of ROMA II Robot. In: Proceedings of the 9th International Conference on Climbing and Walking Robots, pp. 107–114 (2006)
7. Molfino, R., Armada, M., Cepolina, F.: Roboclimber the 3-ton spider. Ind. Rob. **32**(2), 163–170 (2005)
8. Longo, D., Muscato, G.: The Alicia(3) climbing robot. IEEE Rob. Autom. Mag. **13**(1), 42–50 (2006)
9. Savall, J., Avello, A., Briones, L.: Two compact robots for remote inspection of hazardous areas in nuclearpower plants. In: International Conference on Robotics and Automation, ICRA, Detroit, Michigan, USA, May, pp. 1993–1998 (1999)
10. Luk, B., Liu, K., Collie, A., Cooke, D., Chen, S.: Tele-operated climbing and mobile service robots for re-mote inspection and maintenance in nuclear industry. Ind. Rob. Int. J. **33**(3), 194–204 (2006)
11. Armada, M., Prieto, M., Akinfiev, T., Fernandez, R., Gonzalez, P., Garcia, E., Montes, H., Nabulsi, S., Pon-ticelli, R., Sarria, J., Estremera, J., Ros, S., Grieco, J., Fernandez, G.: On the design and development of climbing and walking robots for the maritime industries. Marit. Res. **2**(1), 9–32 (2005)
12. Chu, B., Jung, K., Han, C.S., Hong, D.: A survey of climbing robots: locomotion and adhesion. Int. J. Precis. Eng. Manufact. **11**(4), 633–647 (2010)
13. Schmidt, D., Berns, K.: Climbing robots for maintenance and inspections of vertical structures, a survey of design aspects and technologies. Rob. Autonom. Syst. **61**(12), 1288–1305 (2013)
14. Tummala, R.L., Mukherjee, R., Aslam, D., Dulimarta, H., Minor, M., Dangi, G.: Climbing the walls. IEEE Robot. Autom. Mag. **9**(4), 10–19 (2002)
15. Zhu, H., Guan, Y., Wu, W.: Autonomous pose detection and alignment of suction modules of a bipedwall-climbing robot. IEEE-ASME Trans. Mechatron. **20**(2), 653–662 (2015)
16. Guan, Y., Zhu, H., Wu, W., Zhou, X., Jiang, L., Cai, C., Zhang, L., Zhang, H.: A modular biped wall-climbing robot with high mobility and manipulating function. ASME Trans. Mechatron. **18**(6), 1787–1798 (2013). IEEE

17. Zhao, Y., Fu, Z., Cao, Q., Wang, Y.: Development and applications of wall-climbing robots with a single suction cup. Robotica **22**, 643–648 (2004)

18. Schmidt, D., Hillenbrand, C., Berns, K.: Omnidirectional locomotion and traction control of the wheel-driven, wall-climbing robot, CROMSCI. Rob. J **29**(7), 991–1003 (2011)

19. Koo, I.M., Trong, T.D., Lee, Y.H., Moon, H., Koo, J., Park, S.K., Choi, H.R.: Development of wall climbing robot system by using impeller type adhesion mechanism. J. Intell. Rob. Syst. **72**(1), 57–72 (2013)

20. Qian, Z., Zhao, Y., Fu, Z., Wang, Y.: Fluid model of sliding suction cup of wall-climbing robots. Int. J. Adv. Rob. Syst. **3**(3), 275–284 (2006)

21. Zhou, Q., Li, X.: Experimental comparison of Drag-wiper and Roller-wiper glass-cleaning robots. Ind. Rob. Int. J. **43**(4), 409–420 (2016)

22. Li, X., Kawashima, K., Kagawa, T.: Analysis of vortex levitation. Exp. Therm. Fluid Sci. **32**(8), 1448–1454 (2008)

23. Li, X., Kagawa, T.: Development of a new noncontact gripper using swirl vanes. Rob. Comput. Integr. Manufact. **29**, 63–70 (2013)

24. Zhao, J., Li, X.: Effect of supply flow rate on performance of pneumatic non-contact gripper using vortex flow. Exp. Therm. Fluid Sci. **79**, 91–100 (2016)